A Novel Microtubule-based Motor Protein (KIF4) for Organelle Transports, Whose Expression Is Regulated Developmentally

Yoko Sekine, Yasushi Okada, Yasuko Noda, Satoru Kondo, Hiroyuki Aizawa, Reiko Takemura,* and Nobutaka Hirokawa

Department of Anatomy and Cell Biology, School of Medicine, University of Tokyo, Hongo, Bunkyo-ku, Tokyo 113, Japan; and *Okinaka Memorial Institute for Medical Research, Toranomon, Minatoku, Tokyo 105, Japan

Abstract. To understand the mechanisms of transport for organelles in the axon, we isolated and sequenced the cDNA encoding KIF4 from murine brain, and characterized the molecule biochemically and immunocytochemically. Complete amino acid sequence analysis of KIF4 and ultrastructural studies of KIF4 molecules expressed in Sf9 cells revealed that the protein contains 1,231 amino acid residues (M_r 139,550) and that the molecule (116-nm rod with globular heads and tail) consists of three domains: an NH_2-terminal globular motor domain, a central α-helical stalk domain and a COOH-terminal tail domain. KIF4 protein has the property of nucleotide-dependent binding to microtubules, microtubule-activated ATPase activity, and microtubule plus-end-directed motility. Northern blot analysis and in situ hybridization demonstrated that KIF4 is strongly expressed in juvenile tissues including differentiated young neurons, while its expression is decreased considerably in adult mice except in spleen. Immunocytochemical studies revealed that KIF4 colocalized with membranous organelles both in growth cones of differentiated neurons and in the cytoplasm of cultured fibroblasts. During mitotic phase of cell cycle, KIF4 appears to colocalize with membranous organelles in the mitotic spindle. Hence we conclude that KIF4 is a novel microtubule-associated anterograde motor protein for membranous organelles, the expression of which is regulated developmentally.

THE neuron is a highly polarized cell composed of dendrites, a cell body, and a long axon. Because of the lack of protein synthesis machinery in the axon, proteins necessary in the axon or synapses must be transported down the axon. In this way, the neuron is an excellent model system for studying the mechanisms of intracellular organelle transport. In the anterograde axonal transport, there are two distinct flows: the fast flow that transports most of the membranous organelles, and the slow flow that transports cytoskeletal components (Grafstein and Forman, 1980). Electron microscopic observations of axons have identified crossbridge structures between microtubules and membranous organelles as candidates for organelle transporters (Hirokawa, 1982; Miller and Lasek, 1985; Hirokawa and Yorifuji, 1986; Hirokawa et al., 1989). Some of these crossbridges could be the two previously identified molecular motors, kinesin and brain dynein. Kinesin generates movement along a microtubule for its plus-end (Brady, 1985; Vale et al., 1985*a*,*b*), and it localizes on anterogradely transported organelles in the axon (Hirokawa et al., 1991); it is thus considered to be an anterograde motor. In contrast, brain dynein moves along a microtubule for its minus-end, and is thus considered to be a retrograde motor (Lye et al., 1987; Paschal and Vallee, 1987; Schnapp and Reese, 1989; Schroer et al., 1989; Hirokawa et al., 1990; Koonce et al., 1992; Minami et al., 1993; Zhang et al., 1993).

Kinesin consists of two heavy chains and several light chains (Bloom et al., 1988; Kuznetsov et al., 1988; Hirokawa et al., 1989). Kinesin heavy chain (KHC)[1] consists of an NH_2-terminal globular motor domain that has a putative ATP-binding site and a microtubule-binding site, a central α-helical coiled coil stalk domain, and a COOH-terminal fan-like domain that interacts with light chains and vesicles (Hirokawa et al., 1989; Scholey et al., 1989; Yang et al., 1989). The NH_2-terminal domain of KHC expressed in bacterial cells was shown to move microtubules in vitro (Yang et al., 1990).

Recently, genes encoding kinesin-related proteins were identified in various species of organisms such as *Aspergillus nidulans*, *Saccharomyces cerevisiae*, *Drosophila melanogaster*, *Schizosaccharomyces pombe*, *Caenorhabditis elegans*, *Xenopus leavis*, sea urchin, and human (see review, Goldstein, 1991). All these kinesin-related proteins have do-

Address all correspondence to N. Hirokawa, Dept. of Anatomy and Cell Biology, School of Medicine, University of Tokyo, Bunkyo-ku, Hongo, Tokyo 113 Japan. Tel.: 81 3 3812 2111, ext. 3326. Fax: 81 3 5689 4856.

1. *Abbreviations used in this paper*: CLSM, confocal laser scanning microscope; KHC, kinesin heavy chain; Sf9, *Spodopetra frugiperda*.

© The Rockefeller University Press, 0021-9525/94/10/187/15 $2.00

mains similar to the KHC motor domain. Among them, KAR3, KIP1, and CIN8 proteins were demonstrated to be capable of microtubule-binding in vivo (Meluh and Rose, 1990; Saunders and Hoyt, 1992), and ncd, KRP85/95, Eg5, and MKLP-1 proteins were shown to have motility activity in vitro (McDonald et al., 1990; Cole et al., 1992; Nislow et al., 1992; Sawin et al., 1992*a*; Chandra et al., 1993). No significant sequence similarity was detected in those proteins except for the motor domain, and these unique regions are thought to interact with cargoes carried by these motor proteins. All the members of the kinesin superfamily previously identified participated in mitosis or meiosis except Uncl04, which was thought to play a role in synaptic vesicle transport in neurons in *C. elegans*.

In neurons, various kinds of intracellular components (such as mitochondria, precursors of synaptic vesicles, precursors of axonal plasma membranes, dense cored vesicles, etc.) are transported along microtubules at different velocities and directions in axons or dendrites, and are delivered to their proper destinations (Grafstein and Forman, 1980; Hirokawa et al., 1990, 1991). Our structural studies revealed several different kinds of crossbridge structures between microtubules and membranous organelles (Hirokawa, 1982, 1993; Hirokawa and Yorifuji, 1986). Thus, it is likely that new motors besides the two previously identified ones, kinesin and brain dynein, are necessary to carry several different kinds of organelles at different velocities and directions. To understand the mechanisms of organelle transport further, we recently identified five members of the kinesin superfamily (KIF1-5) in the murine central nervous system by PCR technique (Aizawa et al., 1992).

In this study, we isolated cDNA clones of KIF4 from the mouse brain cDNA library, and revealed that KIF4 is a novel microtubule-based plus-end directed motor protein for membranous organelle transport in juvenile tissues, the expression of which is developmentally regulated.

Materials and Methods

Cloning of KIF4 cDNA

Preparation of the λgt10 cDNA library from poly(A)$^+$ RNA of 5-d-old murine brains and amplification of KIF4 cDNA fragment was performed as previously described (Aizawa et al., 1992). To isolate a complete cDNA clone for KIF4, we screened 5×10^5 independent clones of the 5-d-old murine brain cDNA library using the ^{32}P-labeled KIF4 cDNA fragment (pKIF4; 486 bp) as a probe (see Fig. 1 *a*). Hybridization was performed by established method (Maniatis et al., 1982). We obtained a positive clone (λKIF403) of 4.5 kbp in length. The EcoRI insert of the positive clone was subcloned into the EcoRI site of the pUC18 plasmid vector (Takara, Kyoto, Japan), and the nucleotide sequences of both strands were determined by the dideoxy chain-termination method (Sanger et al., 1977). Next, BstXI/NcoI fragment (K4BN) and BstXI/HindIII fragment (K4BH) within the λKIF403 cDNA insert were also used as probes for screening, and two overlapping clones (λKIF4m and λKIF4c) were obtained (Fig. 1 *a*). Using EcoRI/SmaI fragment (K4ES) as a probe, several positive clones which covered the 5′ region of λKIF403 were obtained (data not shown).

Phylogenetic Analysis of Kinesin Superfamily

The phylogenetic tree of the head sequences of the kinesin superfamily proteins, and the alignment and distance matrix used to generate it were produced using the CLUSTAL V program (Higgins et al., 1992), which uses the neighbor-joining method of Saitou and Nei (1987). The region between IFAYGQT and LAGSE was used for this tree. The sequences used to generate the tree were obtained from GenBank and PIR databases and some references.

Preparation of Recombinant Baculovirus

KIF4 cDNA insert encoding the entire coding region of KIF4 was excised by digestion with KpnI and EcoRI from pUC18 and made blunt ends with Klenow fragment. The fragment was inserted into the SmaI site of pAcYM1 transfer vector, which contains viral polyhedrin promotor for expression of the cloned cDNA insert (Matsuura et al., 1986). The insect cell line Spodopetra frugiperda (Sf9) was maintained in TC-100 medium (GIBCO BRL, Gaithersburg, MD) supplemented with bactotryptose broth and 10% fetal calf serum at 27°C as described (O'Reilly et al., 1992). To obtain recombinant baculovirus containing KIF4 cDNA, Sf9 cells were cotransfected with BaculoGold virus DNA (PharMingen, San Diego, CA) and pAcYM1 carrying KIF4 cDNA. Recombinant virus was purified by end-point dilution assay (O'Reilly et al., 1992), and amplified by four successive infections at 0.1 multiplicity of infection (MOI) to obtain high titration (10^7 plaque-forming units/ml) stock, which was used to infect a monolayer or suspension culture of Sf9 cells for the recombinant KIF4 expression.

Purification of Recombinant KIF4 Protein from Sf9

Sf9 cells infected by recombinant baculovirus at about 10 MOI were harvested at 72 h after infection. All procedures below were performed on ice or at 4°C to prevent proteolysis. After washing with SF9-PBS (1 mM Na_2PO_4, 10.5 mM KH_2PO_4, 140 mM NaCl, and 40 mM KCl, pH 6.2), cells (10^{10} cells packed in 5 ml vol) were suspended with 15 ml PHEM (50 mM Pipes, 50 mM Hepes, pH 7.2, 1 mM EGTA, 1 mM $MgCl_2$, and 5 mM DTT) containing protease inhibitors (1 mM phenylmethylsulfonylfluoride, 1 μg/ml pepstatin A, 10 μg/ml leupeptin, and 10 μg/ml tosyl arginine methyl ester). Cells were homogenized with a teflon-glass homogenizer, and clarified by centrifugation at 150,000 *g* for 30 min. The supernatant was incubated on ice for 30 min after the addition of 1 mM AMP-PNP, 0.3 mg/ml tubulin, and 30 μM taxol. Tubulin was purified from porcine brain as described (Shelanski et al., 1973). The sample was centrifuged at 100,000 *g* for 60 min, and the pellet was resuspended with PHEM containing 10 mM MgATP and 200 mM KCl. After the addition of 30 μM taxol, the sample was incubated at 4°C for 10 min, and centrifuged at 100,000 *g* for 60 min. The supernatant was overlaid on a 5–20% sucrose density gradient solution and centrifuged at 120,000 *g* for 18 h. Fractions were analyzed by SDS-PAGE, ATPase activity and in vitro motility assay. KIF4 sedimented slightly slower than conventional kinesin, and the authentic insect cell motor was enriched in a slightly heavier fraction (see fraction 5 in Fig. 3 *b*) than KIF4 (fraction 7). The heaviest KIF4 fraction (fraction 6), therefore, was discarded to avoid the contamination of the authentic Sf9 motor. The peak KIF4 fraction (fraction 7) was applied to a Sepharose Q fast flow (Pharmacia LKB Nuclear, Gaithersburg, MD) anion exchange column equilibrated with PHEM buffer, and eluted with 20 ml of linear salt gradient (100–300 mM NaCl). KIF4 was eluted ~150 mM NaCl (see fractions 4 and 5 in Fig. 4 *c*), and trace amount of authentic motor was eluted with more than 250 mM NaCl. The purest KIF4 fraction (fraction 4) was pooled and dialyzed against PHEM, and clarified by centrifugation at 100,000 *g* for 15 min. Protein concentration was determined by Bradford's method (Bradford, 1976) with bovine serum albumin as the standard. This fraction was used for the analysis of ATPase activity, motility, and single molecule structure.

ATPase Activity Assay

The ATPase activity was measured by the method of Seals et al. (1978) with some modifications (Maeda et al., 1992). The reaction was started by the addition of 10 μl of 10 mM ATP ([γ-^{32}P]ATP) to solution (90 μl) containing KIF4 (0.1 mg/ml) in the presence or absence of taxol-microtubule (0.1 mg/ml). After incubation at 25°C for 10 min, the reaction was stopped by the addition of 10 μl of 10% SDS to the solution. Free phosphate was separated from [γ-^{32}P]ATP by organic extraction as a phosphomolybdate complex generated by adding 100 μl of phosphate reagent (2 vol of 10 N H_2SO_4, 2 vol of 10% (wt/vol) ammonium molybdate and 1 vol of 0.1 M silicotungstic acid) to the terminated reaction mixture. The organic phase was removed for liquid scintillation counting.

Motility Assay

The motility assay was performed as described previously (Schnapp, 1986; Howard et al., 1989). All procedures were performed at 25°C in PHEM buffer containing 2 mM ATP with casein-coated coverslips. KIF4 (~1 mg/ml) was incubated for 5 min on the cover glass. The movement of taxol-stabilized microtubules (50 μg/ml tubulin and 10 μM taxol) or salt-extracted *Chlamydomonas axonemes* (~0.1 mg/ml) (Witman, 1986; Paschal and

Vallee, 1993) was observed by VEC-DIC microscopy using an Axiophot microscope, a Planneofluor ×100 NA 1.30 objective (Zeiss, Thornwood, NJ), and an Argus10 image processor (Hamamatsu, Bridgewater, NJ). The image was recorded with a EVO-9650 Hi8 videotape recorder (Sony, Tokyo, Japan).

Low-angle Rotary-shadowing EM

Low-angle rotary-shadowing EM was performed as described previously (Hiroakwa et al., 1989). Purified KIF4 (0.1 mg/ml) was adjusted to 0.5 M ammonium acetate and 30% (vol/vol) glycerol in 20 mM Pipes (pH 6.9), 1 mM EGTA and 1 mM $MgCl_2$. This mixture was then sprayed onto freshly cleaved mica flakes, which were subsequently dried under a vacuum. Rotary-shadowing with platinum was performed at an angle of 6° using a Balzers model 301 freeze fracture apparatus (Balzers, Hudson, NH), and the replicas were observed with a JEOL 2000EX electron microscope at 120 kV. The dimensions of various domains of KIF4 molecules were determined by quantitative morphometric methods as described previously (Hirokawa et al., 1989).

Northern Hybridization

Total RNA was prepared from neonatal, 5-d-old, 14-d-old, and adult murine tissues (brain, kidney, liver, spleen, lung, heart, and testis) by the guanidium isothiocyanate/cesium chloride method (Maniatis et al., 1982). Poly(A)$^+$ RNA was purified by oligo (dT) cellulose column chromatography (Maniatis et al., 1982). RNA was quantified by measuring the absorbance at 260 nm, and integrity and amount of the loaded RNA was checked by staining with ethidium bromide following agarose gel electrophoresis. The RNA sample was denatured and electrophoresed in an agarose gel containing 2.2 M formaldehyde. After electrophoresis, the RNA was transferred to a nylon filter (Hybond™-N$^+$, Amersham Inc., Arlington Heights, IL) and cross-linked by UV irradiation. The cDNA fragment of pKIF4 (KIF4A), HindIII/HindIII fragment (KIF4C) within the KIF4 cDNA insert, and a PCR fragment of KHC were used (Fig. 1 *a*). These probes were labeled by a multiprime DNA labeling system as hybridization probes. Hybridization was carried out at 65°C for 8 h in a rapid hybridization buffer (Amersham Inc.). The filters were washed in 0.1× SSC-0.1% SDS at 65°C for 30 min and exposed to x-ray film.

In Situ Hybridization

Adult and 5-d-old mice were fixed by perfusion with 2% paraformaldehyde in 0.1 M phosphate buffer (pH 7.2). The cerebra and cerebella of 5-d-old mice and the spleens of adult mice were then removed and fixed for two additional hours at 4°C. Then the samples were processed as described previously with some modifications (Takemura et al., 1991; Aizawa et al., 1992). As a probe, the NcoI/BstXI (KIF4B) and HindIII/HindIII fragments (KIF4C) within the KIF4 cDNA insert were used. ^{35}S-labeled probes were generated using the hexanucleotide priming method.

Cell Culture

L cells (mouse fibroblast cell line) were cultured in Dulbecco modified eagle medium (GIBCO BRL) containing 10% fetal calf serum. P19 cells (mouse embryonic carcinoma cell line) were cultured and differentiated into neural cells by retinoic acid (10^{-7} M) as described previously (Rudnicki and McBurney, 1987; Tanaka et al., 1992).

Antibody Preparation

Anti-KIF4 antisera were obtained from rabbits into which purified KIF4 protein from Sf9 cells was injected as antigen. Anti-KIF4 antibody was further affinity-purified from the antisera by the method of Olmsted (1981) using recombinant KIF4 protein purified from bacterial cells. The expression plasmid for the recombinant KIF4 protein (p11J) was constructed as follows. A 3.0-kb DraI/BamHI fragment of KIF4 cDNA was inserted into a pET3d vector (Novagen, Inc., Madison, WI). The plasmid p11J encodes the polypeptide of KIF4 (amino acids residues 78–1,071) with an additional methionine residue on its NH_2-terminal and an additional 20 residues (RLLTKPERKLSWLLPPLSNN) on the COOH-terminal. The recombinant KIF4 protein was expressed by *E. coli* strain BL21 (DE3) pLysS carrying the p11J plasmid in minimal medium M9ZB (Studier et al., 1990) supplemented with 100 μg/ml ampicillin and 1 mM isopropyl-beta-D-thiogalactopyranoside at 37°C for 3 h. The bacterial cells were harvested by centrifugation, suspended in 100 mM Pipes (pH 6.8), 2 mM EGTA, and 1 mM $MgCl_2$, and sonicated. The expressed KIF4 polypeptide was purified from inclusion bodies as described previously (Harlow and Lane, 1988).

Immunoblot

After gel electrophoresis, proteins were transferred onto Immobilon™ membrane (Millipore Corp., Bedford, MA) as described (Towbin, 1979). The membrane was stained by anti-KIF4 antibody using HRP-conjugated goat anti-rabbit antibody as a second antibody or ^{125}I-protein A for quantitative experiments.

Subcellular Fractionation

Cultured cells were homogenized in 9 vol of solution containing 250 mM sucrose, 10 mM Hepes (pH 7) and a cocktail of the protease inhibitors by teflon homogenizer. The homogenate was sequentially centrifuged at 600 *g* for 10 min, 5,000 *g* for 10 min, 8,000 *g* for 10 min, and 100,000 *g* for 60 min to collect pellets as nuclear, heavy mitochondria, light mitochondria (5,000–8,000 *g*), and microsomal fractions (100,000 *g*), respectively. The final supernatant was also collected as a soluble fraction.

Immunocytochemistry

Cells were rinsed with PBS (10 mM sodium phosphate buffer, pH 7.4, 150 mM NaCl), fixed with 2% paraformaldehyde and 0.1% glutaraldehyde in PBS, and then permeabilized with 0.5% Triton X-100 in PBS. If necessary, cells were permeabilized for 5 min at 37°C with 0.02% saponin in PEM supplemented with 10 μM taxol before fixation with 2% paraformaldehyde in PEM in the presence of 10 μM taxol and 0.5% Triton X-100. After brief washes with PBS, the fixative was quenched with 50 mM glycine in PBS. The cells were then incubated with the blocking solution (10% normal goat serum and 5% bovine serum albumin in PBS), followed by incubation with primary antibodies. As primary antibodies, affinity-purified anti-KIF4 antibodies, anti-tubulin monoclonal antibodies (DM1A; Amersham Corp., Westbury, NY) and anti-neurofilament M monoclonal antibodies (NN18; Boehringer Mannheim Corp., Indianapolis, IN) were used. Normal rabbit IgG, preimmune serum, and affinity-purified antisera absorbed with KIF4 were used as controls. Rhodamine-conjugated goat anti-rabbit immunoglobulins (Cappel Laboratories, Cochranville, PA) and FITC-conjugated goat anti-mouse immunoglobulins (Amersham Corp.) were used as second antibodies. After coverslips were mounted with 50% glycerol and 50 mg/ml 1,4-diazobicyclo[2,2,2]-octane (Sigma Chem. Co., St. Louis, MO) in PBS (pH 8.6), the samples were observed with an Axiophot microscope (Zeiss). Some samples were observed with a confocal laser scanning microscope (CLSM) (LSM410; Zeiss).

Electrophoresis

SDS-PAGE was performed according to the method of Laemmli (Laemmli, 1970) using 7.5% (wt/vol) polyacrylamide gels. Molecular weight markers used were purchased from BioRad (Richmond, CA). Gels were stained with 0.1% Coomassie blue R.

Chemicals

Taxol was generously supplied by Dr. N. R. Lomax (Natural Product Branch, Division of Cancer Treatment, National Cancer Institute, Bethesda, MD). All other chemicals used were of reagent grade.

Results

Isolation and Characterization of KIF4 cDNA Clones

We isolated a KIF4 cDNA clone (λKIF403) of 4.5 kbp in length as described in Materials and Methods. Northern blot analysis using KIF4 cDNA fragments KIF4A and KIF4C demonstrated that the KIF4 transcript was 4.5 kbp in length (see Fig. 8). Since the size of the largest clone, λKIF403, approximately corresponded to that of the KIF4 transcript (4.5 kbp), we supposed that λKIF403 contained a full length of the KIF4 transcript. Then, we determined the nucleotide and predicted amino acid sequence of KIF4 (Fig. 1 *b*). λKIF403 was found to encode a single open reading frame of 3,693

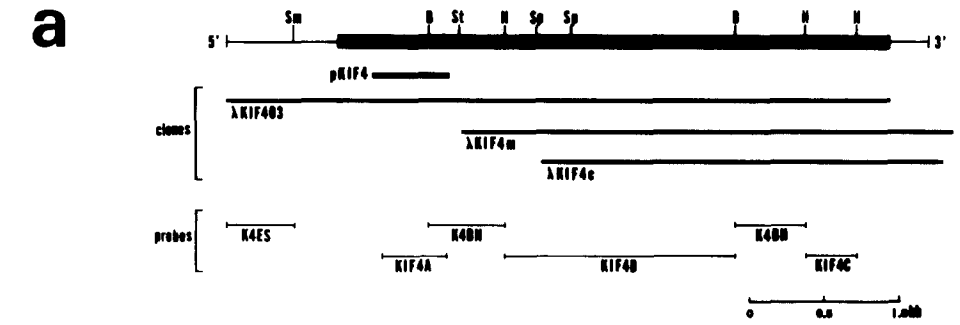

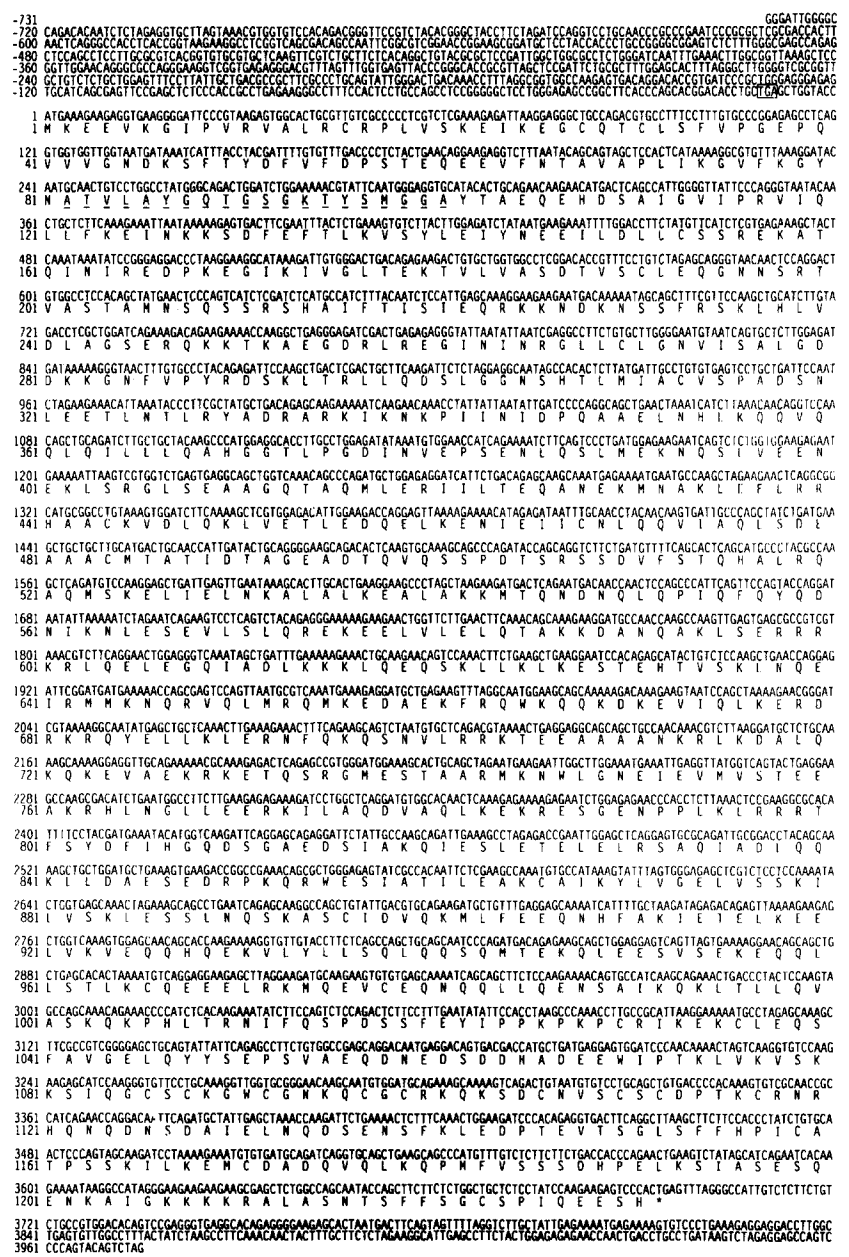

Figure 1. Nucleotide and predicted amino acid sequence of KIF4. (*a*) Restriction map and overlapping cDNA clones of KIF4. An open reading frame of 3,693 nucleotides in length (*thick line*) and 5'- and 3'-flanking regions (*thin line*) are shown at the top. Cleavage sites of several restriction enzymes are shown as follows: *Sm*, SmaI; *B*, BstXI; *H*, HindIII; *N*, NcoI; *P*, PstI; *Sp*, SphI; *St*, StuI. Regions included in cDNA clones and the fragment amplified by PCR (*pKIF4*) are shown in the middle. The fragments used as probes for screening of cDNA cones (*K4BN* and *K4BH*), Northern blot analysis (*KIF4A* and *KIF4C*) and in situ hybridization (*KIF4B* and *KIF4C*) are shown at the bottom. (*b*) Complete nucleotide sequence and deduced amino acid sequence of KIF4. Nucleotide residues are numbered beginning with the first letter of the initiation codon. The initiation methionine codon follows an in-frame termination codon (*box*). The putative ATP-binding site in the motor domain is indicated by a broken underline. The stop codon is marked with an asterisk. This sequence has been submitted to GenBank/DDBJ under accession number D12646.

nucleotides in length. Thus, KIF4 is predicted to consist of 1,231 amino acid residues with a relative molecular mass of 139,550.

The diagonal dot matrix comparison of KIF4 and *Drosophila* KHC (Yang et al., 1989) demonstrated the KIF4 contained an NH_2-terminal domain (amino acid residues 1–350) whose primary sequence is significantly similar to the NH_2-terminal motor domain of KHC, which is known to generate movements along microtubules. The other region of KIF4 displays less significant identity with KHC and other

members of the kinesin superfamily. These data indicated that KIF4 is a novel member of the kinesin superfamily. According to the secondary structure prediction of the Chou-Fasman and Robson-Garnier methods (Chou and Fasman, 1974; Garnier et al., 1978), the NH_2-terminal motor domain (amino acid residues 1–350) is considered to be a globular structure. The central domain (amino acid residues 351–1,005) is predicted to contain three large α-helical rod structures (residues 401–489, 554–750, and 811–1,005). Among the three, two helices (residues 401–489 and 811–1,005) showed the characteristic heptapeptide-repeats d, e, f, g, a, b, c with enrichment of hydrophobic residues at positions d and a, while the other helix (residues 554–750) did not (Fig. 2). Thus it is predicted that the α-helical stalk domain is able to produce the coiled-coil structure with another molecule. The COOH-terminal domain (amino acid residues 1,006–1,231) is predicted to form a globular structure, and contains significantly abundant Ser residues (13.8%).

Phylogenetic Analysis of KIF4 and Other Kinesin Superfamily Proteins

To analyze the structural relationship of motor proteins, we have conducted an amino acid sequence comparison among head domains of kinesin superfamily proteins (between the conserved IFAYGQT and LAGSE) using a distance matrix and the neighbor-joining method (Saitou and Nei, 1987; Fig. 3). In the rootless phylogenetic tree generated by this procedure, the distance along the branches connecting two sequences is a measure of the percent difference in their amino acid sequence. The tree demonstrated that kinesin superfamily contains at least seven families and several other outgroups. This classification was confirmed by the fact that the sequence homology in the region outside the motor domain was not significant between the different families, while it was highly significant among the members belonging to the same family.

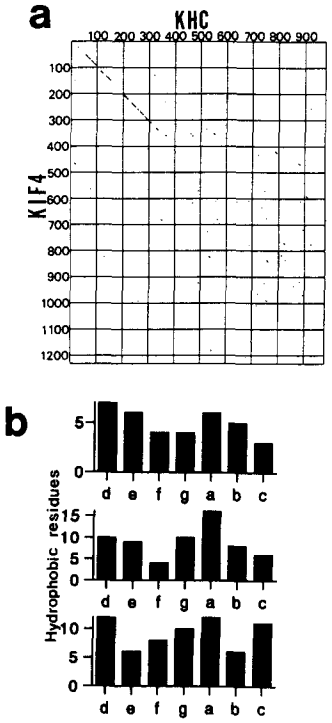

Figure 2. Diagnonal dot matrix and the predicted secondary structure of KIF4. (*a*) Diagonal dot matrix comparison between KIF4 and KHC was performed using an SDC-GENETYX computer program. The dots correspond to the midpoints of 15-residue spans, giving a double-matching probability that the mean score is >2.0. The sequence of KHC was quoted from Yang et al. (1989). (*b*) Periodicities of hydrophobic amino acids were examined in the predicted α-helical region of the central domain. Hydrophobic residues between 401 and 489 (*top*), 554 and 750 (*middle*), and 811 and 1,005 (*bottom*) are shown.

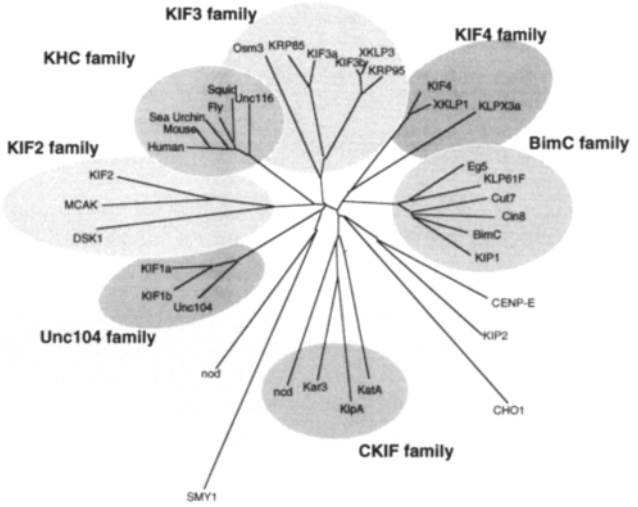

Figure 3. Phylogenetic analysis of kinesin superfamily proteins. The sequences of the fragments of the head motor domains of kinesin superfamily proteins were aligned, and the genetic distance was calculated. Then the phylogenetic tree was drawn by NJ method as described in Materials and Methods. Seven families (*shaded*) were identified in >800/1000 bootstrapping, and further confirmed by the sequence comparison outside the conserved motor domain. Thus there are at least seven families in kinesin superfamily: five NH_2-terminal motor type families (Unc104 family, KHC family, KIF3 family, KIF4 family and BimC family), one central motor type KIF2 family and one COOH-terminal motor type CKIF family. Most of the sequences used for the alignment were obtained from the GenBank data base. Their accession numbers are as follows; KIF1B: D17577; Unc104: M58582; KIF2: D12644; KHC (human): X65873; KHC (mouse): X61435; KHC (sea urchin); X56844; KHC (*Drosophila*): M24441; KHC (squid): J05258; Unc116: L19120; Osm3: D14968; KRP85: L16993; KIF3A: D12645; KRP95: U00996; KLPX3a: L19117; Eg5: X54002; KLP61F: U01842; Cut7$^+$: X57513; CIN8: Z11859; BimC: M32075; KIP1: Z11962; ENP-E: Z15005; KIP2: Z11963; CHO1: X67155; KatA: D11371; KlpA: X64603; KAR3: M31719; ncd: M33932; SMY1: M69021; nod: M36195. PIR accession numbers are as follows; KIF1A: E44259, XKLP1:A48835, XKLP3: C48835. The sequence of KIF3B is unpublished data of our laboratory (H. Yamazaki, personal communication). The sequences of DSK1 and MCAK were obtained by generous personal communications from W. H. Cande and L. Wordeman, respectively.

COOH-terminal motor domain type proteins such as ncd and KAR3 were all categorized in one family, and here we call it as CKIF (C-terminal motor type Kinesin superFamily protein) family. The central motor domain type proteins like KIF2 were also classified into one family, KIF2 family. And the remaining five families have motor domain at their NH_2-terminal.

Before our report on KIF4, four NH_2-terminal motor type families were recognized: KHC family, BimC family, Unc104 family, and KIF3 family (Goldstein, 1993). KIF4 showed low homology to anyone of the four families. However, recently reported *Xenopus* KIF XKLP1 (Vernos et al., 1993) showed significant similarity (identity 80%, similarity 93%) to KIF4 in its motor domain (only partial sequence was available). And *Drosophila* KIF KLPX3a (William, B. C., E. V. William, T. B. Chou, N. Perrimon, and M. L.

Goldberg, unpublished data. GenBank accession number L19117) also showed relatively high similarity to KIF4 even outside the motor domain (identity 31%, similarity 58%), although this value means that KLPX3a could not be a *Drosophila* homologue of KIF4. Thus we consider that the three proteins belong to a new NH_2-terminal motor type family, KIF4 family.

Expression of Recombinant KIF4 in Sf9 Cells and Its Purification

For biochemical and biophysical characterization of KIF4 protein, we examined KIF4 protein with the baculovirus-Sf9 expression system (O'Reilly et al., 1992). This system is considered to produce more native molecules than a bacterial expression system by eukaryotic posttranslational modifications and by correct folding machinery. Recombinant KIF4 protein expressed in Sf9 cells was cosedimented with microtubules in the presence of 2 mM AMP-PNP (Fig. 4 *a*, lane *3*). The pellet was resuspended with PEM containing 10 mM ATP and 200 mM KCl, and KIF4 protein released from the microtubules was collected as the supernatant after centrifugation (Fig. 4 *a*, lane *6*). The release of expressed KIF4 by 10 mM ATP was not efficient in the absence of 200 mM KCl. A control experiment using parent virus infected cells, which express β-galactosidase instead of KIF4, revealed that this fraction contained authentic microtubule dependent motors, probably Sf9 kinesin (data not shown). We further purified the supernatant fraction by sucrose density gradient centrifugation. KIF4 was enriched around fraction 7 (Fig. 4 *b*). Analysis of ATPase activity of each fraction indicated that microtubule-activated ATPase activity was predominantly enriched around fraction 7, corresponding to the KIF4 protein (data not shown). Before this peak, a trace of microtubule-activated ATPase activity was recovered. A control experiment with parent virus showed that this was an authentic motor enriched fraction, and the KIF4 fraction contained only a trace amount of authentic motor. In order to remove the trace amount of Sf9 kinesin from the KIF4 fraction, the fraction was further subjected to anion exchange column chromatography (Q-fast flow). The profile of ATPase activity of the fractions was completely consistent with the protein elution profile of KIF4, suggesting that the final fraction (fraction 4 in Fig. 4 *c*) contained no other ATPase factors than KIF4 (data not shown). We confirmed that Sf9 authentic motors were retained in the columns under the conditions used, and that no ATPase activity was detected in the anion-exchange column chromatography when we used Sf9 cells infected with control virus as a starting material (data not shown).

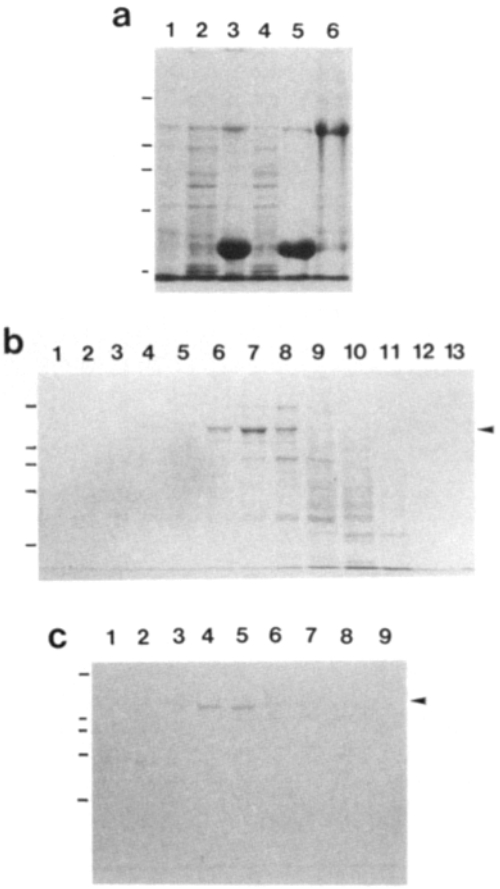

Figure 4. Purification of recombinant KIF4 expressed in Sf9 cells. The pellets (lanes *1*, *3*, and *5*) and supernatants (lanes *2*, *4*, and *6*) of the first three centrifugation steps were analyzed by SDS-PAGE (*a*). KIF4 was concentrated by cosedimentation with microtubules in the presence of AMP-PNP (lane *3*), and released from them by ATP and KCl (lane *6*). This fraction was further purified by sucrose density gradient (SDG). The SDG fraction was analyzed by SDS-PAGE (*b*). Microtubule activated ATPase activity showed one large peak corresponding to the peak of KIF4 protein (lanes *6*, *7*, and *8*). Trace microtubule-activated ATPase activity due to authentic insect cell motor protein was recovered before this peak (lane *5*). To avoid the contamination of authentic motor by the possible overlap of these two peaks, only lane *7* was applied to the anion exchange column. The profile of ATPase activity of the eluate was perfectly consistent with the protein elution profile of KIF4 (*c*). The control experiment showed that the authentic motor was eluted in much later fractions. The purest KIF4 fraction (lane *4*) without even a trace amount of authentic motor contamination was used for the assays. The positions of molecular mass markers (200, 116, 97, 66, and 43 kD) are shown on the left side of the gels, and the position of the KIF4 band is shown on their right side (*arrowhead*).

Microtubule-binding Activity and Motility Assay of KIF4

The primary structure of KIF4 strongly suggested that the molecule is an ATP-dependent motor protein in the microtubule system. In fact, purified KIF4 protein associated and dissociated with microtubules in the presence of AMP-PNP and ATP, respectively (Fig. 5). KIF4 has ATPase activity (6.1 nmol/mg/min), and this activity was activated 35-fold by microtubules (2.1×10^2 nmol/mg/min). Furthermore, we observed the motility of microtubules on KIF4-coated coverslips. At a high concentration of KIF4 (2 mg/ml), microtubules moved 10-fold slower (0.034 ± 0.004 μm/s, $n = 44$) than kinesin (Fig. 6 *A*). At a low concentration of KIF4 (0.2 mg/ml), most microtubules formed bundles and showed no motility (data not shown).

Next, we used axonemes from *Chlamydomonas* flagella to determine the direction of motility (Paschal and Vallee, 1987). Axonemes showed no tendency to form bundles and moved at 0.20 ± 0.02 μm/s ($n = 45$) even with a low concentration of KIF4 (0.1 mg/ml) (Fig. 6 *B*). The speed was 40% of that of kinesin. Almost all axonemes (98/100) moved to-

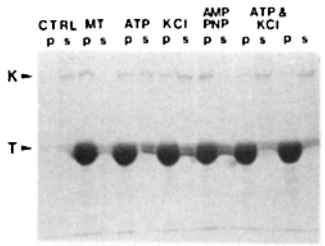

Figure 5. Nucleotide dependent and independent binding of KIF4 to microtubules. Purified recombinant KIF4 was mixed and incubated with polymerized purified microtubule in the presence of nucleotide or salt, and the microtubules were spun down by centrifugation. The pellets (*p*) and the supernatants (*s*) were analyzed by SDS-PAGE. In the control condition (*CTRL*) without microtubules, all KIF4 was recovered in the supernatant, but almost all KIF4 bound to microtubules without exogenous nucleotide (*MT*). The addition of 10 mM ATP (*ATP*) or 150 mM KCl (*KCl*) released about half of KIF4, but 10 mM AMP-PNP (*AMP-PNP*) augmented the binding of KIF4 to microtubules. The combination of 10 mM ATP and 100 mM KCl released most KIF4, and 10 mM ATP and 200 mM KCl released almost all KIF4 (*ATP & KCl*). The positions of KIF4 (*K*) and tubulin (*T*) bands are shown on the left of the gel.

ward the compact (minus) end on KIF4 coated coverslips indicating that KIF4 is a plus-end directed motor protein.

The speed of axoneme was about six times faster than microtubule. This correlates with the KIF4 concentration required to move them; microtubule requires about 10 times concentrated KIF4 than axonemes. Thus, microtubule appears to be a worse substrate for KIF4 than axoneme. For most microtubule dependent motor protein reported to date, however, it is rather difficult to move axonemes than microtubules. What causes this difference? We consider that the bundling of microtubule exerts some drag force against KIF4, which slows or inhibits its movement. Axonemes were not bundled even in the presence of KIF4, and KIF4 could translocate them without any resistance. This speculation was supported by the assay using proteolytically digested KIF4 fragment. The fragment showed no microtubule bundling activity, and translocated microtubules at the same velocity as axonemes (data not shown).

Single Molecule Structure of KIF4

How does KIF4 protein translocate along microtubules using ATP hydrolysis energy? In order to understand the energy conversion mechanism of KIF4, it is essential to have information concerning the ultrastructure of the molecule. Thus, we investigated the single molecular structure of KIF4, especially in comparison with that of kinesin (Hirokawa et al., 1989). Low-angle rotary-shadowing technique revealed a characteristic morphological feature of the KIF4 molecule as summarized in Fig. 7. Most of the KIF4 molecules took on a rod-shaped structure, and each molecule had two globular domains on one end. This two heads and one rod structure is quite similar to the ultrastructure of kinesin (Hirokawa et al., 1989) except for the size of the rod domain. The total length of the KIF4 molecule (116 ± 4 nm, $n = 77$) is longer than that of kinesin (80 nm). The long diameter of the KIF4 head (12 ± 0.6 nm, $n = 53$) is similar to that of kinesin (10 nm). About half of the rod-shaped structure appeared straight, while the rest was bent at the middle of the molecule. The position of the hinge found within the rod-like region was located about 60 ± 10 nm ($n = 30$) from the near edge of the globular heads.

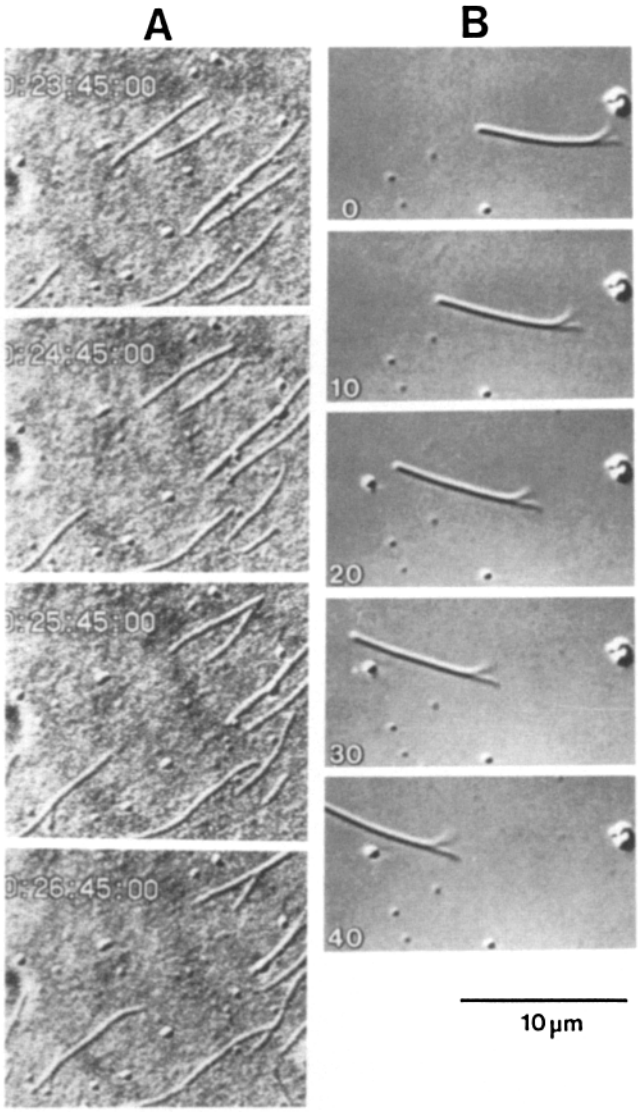

Figure 6. Motility assay of recombinant KIF4. The movement of microtubules (*A*) and axonemes (*B*) on recombinant KIF4-coated coverslips was observed. Most microtubules formed bundles, and moved slowly at a speed of 0.034 μm/s (the time interval in *A* is 1 min). Axonemes were not bundled, and moved at a speed of 0.2 μm/s toward their compact (−) ends (the time interval in *B* is 10 s). Bar, 10 μm.

The head domain of kinesin was previously shown to correspond to the motor domain, and two molecules of kinesin heavy chain were considered to construct the α-helical coiled coil structures corresponding to the rod-like structures (Hirokawa et al., 1989). The primary structure of KIF4 indicates that this protein has putative α-helical coiled coil structures in its central domain. Taking these data together, we conclude that KIF4 protein exists as a parallel α-helical coiled-coil homo dimer with two globular motor domains on its one end. The other end of KIF4 molecule showed an ambiguous filamentous tail structure. Since the tail region of kinesin was considered to be the interaction site of light chains and membrane organelles, this ambiguous structure of the KIF4 tail region might be caused artificially by the absence of its associated proteins in the Sf9 cells.

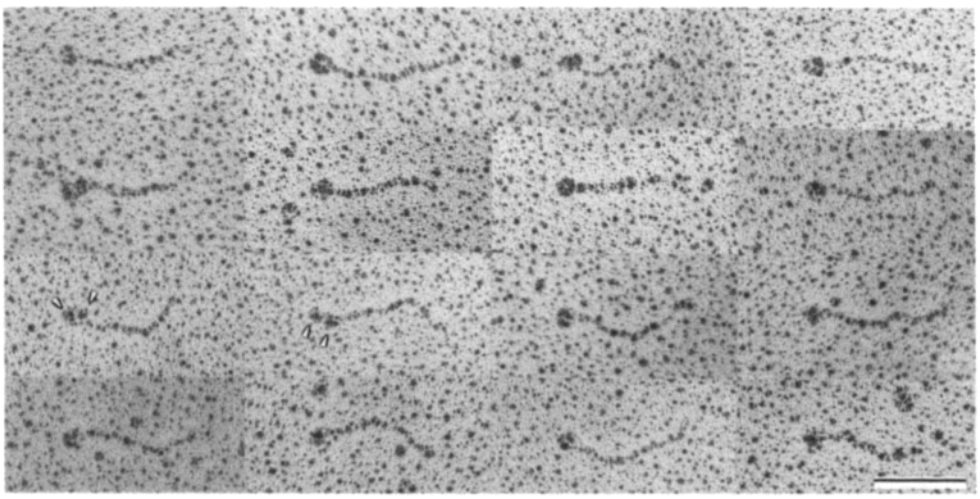

Figure 7. Single molecule structure of recombinant KIF4. Purified recombinant KIF4 was observed after low-angle, rotary-shadowing. Several representative molecules are shown. One or mostly two globular head domains (*arrowheads*) are visible at the left end of each molecule, while less well-defined tail elaborations can be seen on the opposite ends. About half of the molecules observed showed a bend (*lower half*). Bar, 100 nm.

Northern Hybridization of KIF4

Northern blot analysis was performed in order to examine the size, developmental expression, and tissue distribution of the KIF4 transcript (Fig. 8). As probes, KIF4A in the motor domain and KIF4C covering the COOH-terminal domain in addition to the consensus region were used. Both of the probes detected a single transcript of 4.5 kbp in length (Fig. 8 *a*), and the transcript was expressed in murine brain until postnatal day 5. The expression then became gradually weaker, and was almost completely absent in adult brain. In contrast, KHC was expressed constantly throughout murine brain development (Fig. 8 *a*). At postnatal day 0, KIF4 transcript was expressed in all other tissues examined (Fig. 8 *b*). As the mouse grew, the expression of KIF4 decreased in all tissues except the spleen. In the adult mouse, KIF4 was expressed almost exclusively in the spleen tissue, with only a trace amount being expressed in other tissues.

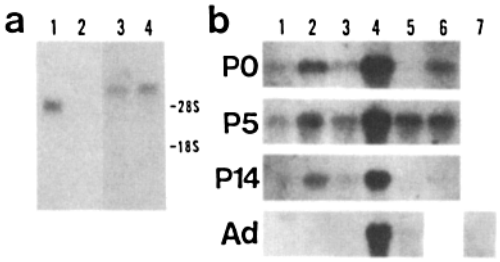

Figure 8. Northern blot analysis of the KIF4 transcript. (*a*) Samples (2 μg) of poly(*A*)$^+$ RNA from 5-d-old (lanes *1* and *3*) and adult (lanes *2* and *4*) murine brains were analyzed using KIF4A (lanes *1* and *2*) and a PCR fragment of KIF5 (lanes *3* and *4*) as probes. (*b*) Samples (10 μg) of total RNA from neonatal (*P0*), 5-d-old (*P5*), 14-d-old (*P14*), and adult (*Ad*) murine tissues, brain (lane *1*), kidney (lane *2*), liver (lane *3*), spleen (lane *4*), lung (lane *5*), heart (lane *6*), and testis (lane *7*) were analyzed using KIF4C as a probe. We checked the size and loaded amounts of the rRNAs as the internal standard markers. The positions of 28S and 18S rRNAs are marked.

In Situ Hybridization of KIF4

To further examine the details of the expression pattern of KIF4 in brain, we performed in situ hybridization. As probes, we selected KIF4B and KIF4C corresponding to nucleotides 1,838–3,375 and 3,116–3,461 of KIF4 cDNA, respectively, both of which show no significant similarity to the other nucleotide sequences. In fact, probe KIF4C can recognize only a single transcript by Northern blot analysis (Fig. 8). We observed the distribution of the KIF4 transcripts in 5-d-old murine brain in comparison with β-actin as control. The expression of KIF4 mRNA was shown to be particularly enriched in the hippocampus and cerebellar cortex (Fig. 9). The KIF4 mRNA was expressed in the CA1, CA2, CA3, and dentate gyrus regions of the hippocampus (Fig. 9, *A* and *C*), as well as in the outer and inner granular layers of the cerebellar cortex (Fig. 9, *B* and *D*). At higher magnification, signals of KIF4 were detected on pyramidal cells in the hippocampus and on granular cells in the cerebellum (Fig. 9, *E* and *F*). β-actin transcripts were detected in all areas of the cerebrum and cerebellum (data not shown; see Takemura et al., 1991). In situ hybridization of KIF4 transcripts in adult brain showed signals of the background level only (data not shown). Therefore, it was concluded that KIF4 was expressed predominantly in young neurons.

Figure 9. Expression pattern of the KIF4 transcript in juvenile murine brain. Transverse sections of the cerebrum (*A* and *C*) and sagittal sections of the cerebellum (*B* and *D*) of 5-d-old mice were hybridized with the cDNA probe KIF4C (*A* and *C*) and a β-actin cDNA (data not shown). Slides were processed by dipping in 1:1 Ilford K-5 emulsion, and were exposed for 2 wk. The developed slides were observed using dark-field optics (*A–D*), or bright field optics after staining with hematoxylin and eosin (*E* and *F*). *CA1*, *CA2*, and *CA3*, areas of hippocampus; *PC*, pyramidal cells; *OGL*, outer granular layer; *IGL*, inner granular layer. Strong expression of KIF4 mRNA is detected in the hippocampus (*C* and *E*) and granule cells in dentate gyrus and inner and outer granule cells in the cerebellum also express KIF4 mRNA abundantly (*D* and *F*). Bars: (*A*) 1 mm; (*B–D*) 100 μm; (*E* and *F*) 10 μm.

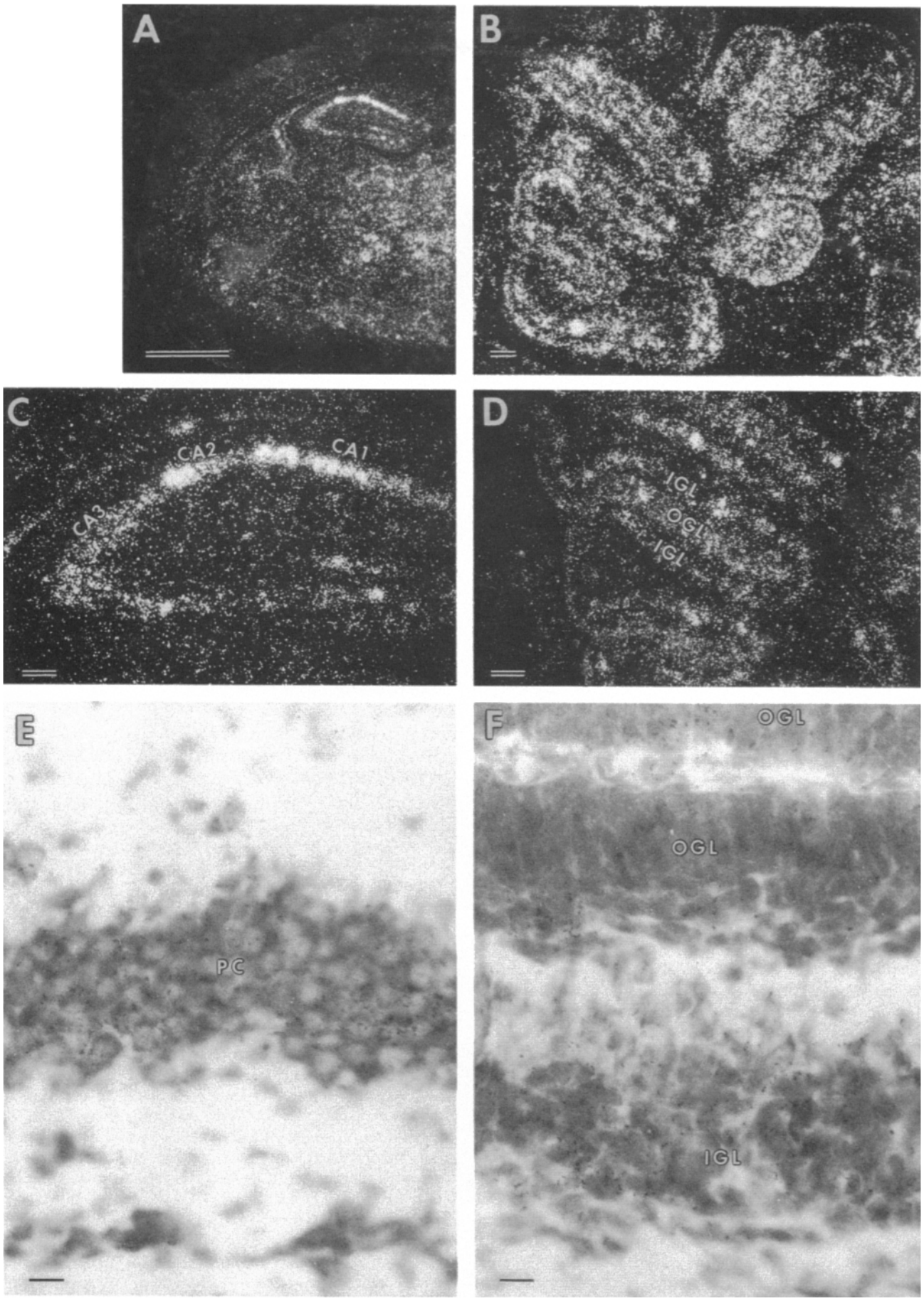
A
B
C
CA2
CA1
CA3
D
IGL
OGL
IGL
E
PC
F
OGL
OGL
IGL

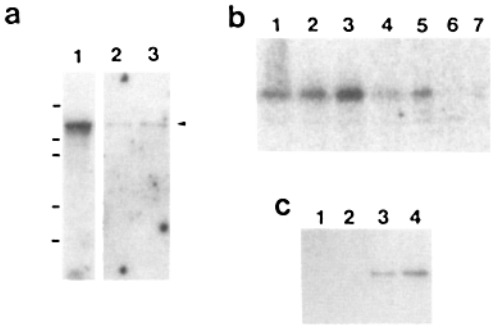

Figure 10. Immunoblot analysis of KIF4 protein. (*a*) The affinity-purified anti-KIF4 antibody stained a single band at the expected position (140 kD) on the immunoblot of the total homogenate of culture cells. KIF4 was abundantly expressed in L cell (lane *1*). The embryonic carcinoma cell line P19 also expressed KIF4 protein (lane *2*). When P19 was induced to differentiate into neuronal cells, the expression of KIF4 increased (lane *3*). Approximately 10^6 cells were homogenized with 1 ml buffer and a 10-μl aliquot was loaded in each lane. (*b*) Immunoblot of the developing murine cerebella. The total homogenate of equal wet weight of cerebella at postnatal 1, 3, 5, 7, 9, 14, and 21 d are applied (1 mg tissue/lane) in lanes 1–7, respectively. The expression of KIF4 in murine cerebellum was transient. The amount of KIF4 increased until postnatal day 5 (lane *3*), and decreased after postnatal day 9 (lane *5*). It was undetectable in the cerebellum of young adult or adult mice. (*c*) Immunoblot of subcellular fractionation of L cells showed that 40–60% of KIF4 binds to the microsomal fraction (lane *3*) and then 40–60% of KIF4 was recovered in the soluble fraction (lane *4*). KIF4 was not detectable in heavy or light mitochondrial fractions (lanes *1* and *2*). Approximately 10^6 cells were homogenized with 1 ml buffer as starting materials. Each fraction by sequential centrifugation was suspended to 1 ml buffer, and an aliquot (10 μl) was loaded in each lane.

Intracellular Localization of KIF4 Protein

What kind of components does KIF4 transport in the cells? To get some insight into the answer to this question, we investigated the intracellular localization of KIF4 in cultured cells. First, we stained mouse L cells with the anti-KIF4 antibody, because L cells express native KIF4 at a high level (Fig. 10 *a*). In interphase cells, the staining with anti-KIF4 antibody showed punctate patterns with vague filamentous staining and diffuse cytoplasmic staining (Fig. 11 *b*). In most cells, we observed also some staining in nuclei. Confocal microscopic observation of a double-stained sample clearly showed that the punctate staining corresponds to some membranous organelles, and that the filamentous staining was colocalized with microtubules (Fig. 11, *d* and *e*). This observation confirmed the idea that KIF4 functions as a microtubule-dependent motor, which transports membranous organelles in interphase cells. In fact, standard subcellular fractionation with sequential centrifugation showed that more than half of KIF4 was recovered in the microsomal fraction, but not in heavy nor light mitochondrial fractions (Fig. 10 *c*).

Next, we investigated the localization of KIF4 in mitotic L cells. Anti-KIF4 antibody stained the mitotic apparatus and also cytoplasmic structures in a punctated fashion (Fig. 12). The punctate staining appeared similar to that in interphase cells, and thus we consider that KIF4 colocalized with small membranous organelles both in interphase and mitotic cells. The staining of the mitotic apparatus colocalized with spindle microtubules suggests the two following possibilities: KIF4 takes part in the sliding of spindle microtubules as a mitotic motor, or KIF4 is bound to membranous organelles enriched along spindle microtubules as shown in the staining with anti-kinesin antibody in sea urchin eggs (Scholey et al., 1985; Wright et al., 1991).

Finally, we examined the intracellular localization of KIF4 protein in juvenile neuronal cells, because the neuron provides a good model system for investigating the mechanism of intracellular organelle transport along microtubules, and because KIF4 is predominantly expressed in juvenile neurons. An embryonic carcinoma cell line, P19, can be induced to differentiate to neuronal cells in vitro, and has been intensively studied for the expression time course of neuronal markers (Tanaka et al., 1992). Therefore we chose this cell line as a model. Immunoblot analysis showed that this cell line expressed KIF4 protein before neural induction, and that the expression increased transiently after neural induction and showed a gradual decrease subsequently (Fig. 10, *a* and *b*). KIF4 protein was detected in neurites and growth cones of growing neurons (36–48 h after neural induction) (Fig. 13 *a*), which were identified as neurons by their morphological characteristics and positive staining with anti-neurofilament antibody (Fig. 13 *b*). Observation of the growth cones at higher magnification demonstrated that KIF4 staining revealed a punctate organelle pattern with vague filamentous staining colocalized with microtubules (Fig. 13, *d* and *f*). These data strongly suggest that KIF4 transports membranous organelles along microtubules to the active growth cones of juvenile neurons.

Discussion

KIF4 Is a Novel Member of Kinesin Superfamily with NH_2-terminal Motor Domain (Heads) and COOH-terminal Tail

The secondary structure prediction of KIF4 from its amino acid sequence suggested that the molecule was composed of three domains: the NH_2-terminal globular motor domain, the central α-helical stalk domain, and the COOH-terminal tail domain. This three domain structure of KIF4 coincides well with the molecular shape of recombinant KIF4 observed by the low-angle rotary-shadowing technique under electron microscopy which indicated that KIF4 works as a homodimer. The COOH-terminal tail domain of KIF4 showed a fine filamentous tail resembling that of KHC under electron microscopic observation. Because the tail of KHC was shown to interact with light chains and organelles (Hirokawa et al., 1989), the structural resemblance of KIF4 and kinesin molecules suggests that the tail region of KIF4 may also interact with other molecules such as light chains and organelles. Although the sequence homology was not significant outside the motor domain, the three domain structure and overall ultrastructure of KIF4 resembles those of KHC and KIF3A/3B except for the length of the central stalk domain (Hirokawa et al., 1989; Kondo et al., 1994; Yamazaki, H., T. Nakata, Y. Okada, and N. Hirokawa, manuscript submitted for publication). This structural resemblance suggests that the mechanisms of the mechanochemical transport systems of these microtubule-based motors (KHC and KIF4) are basically identical.

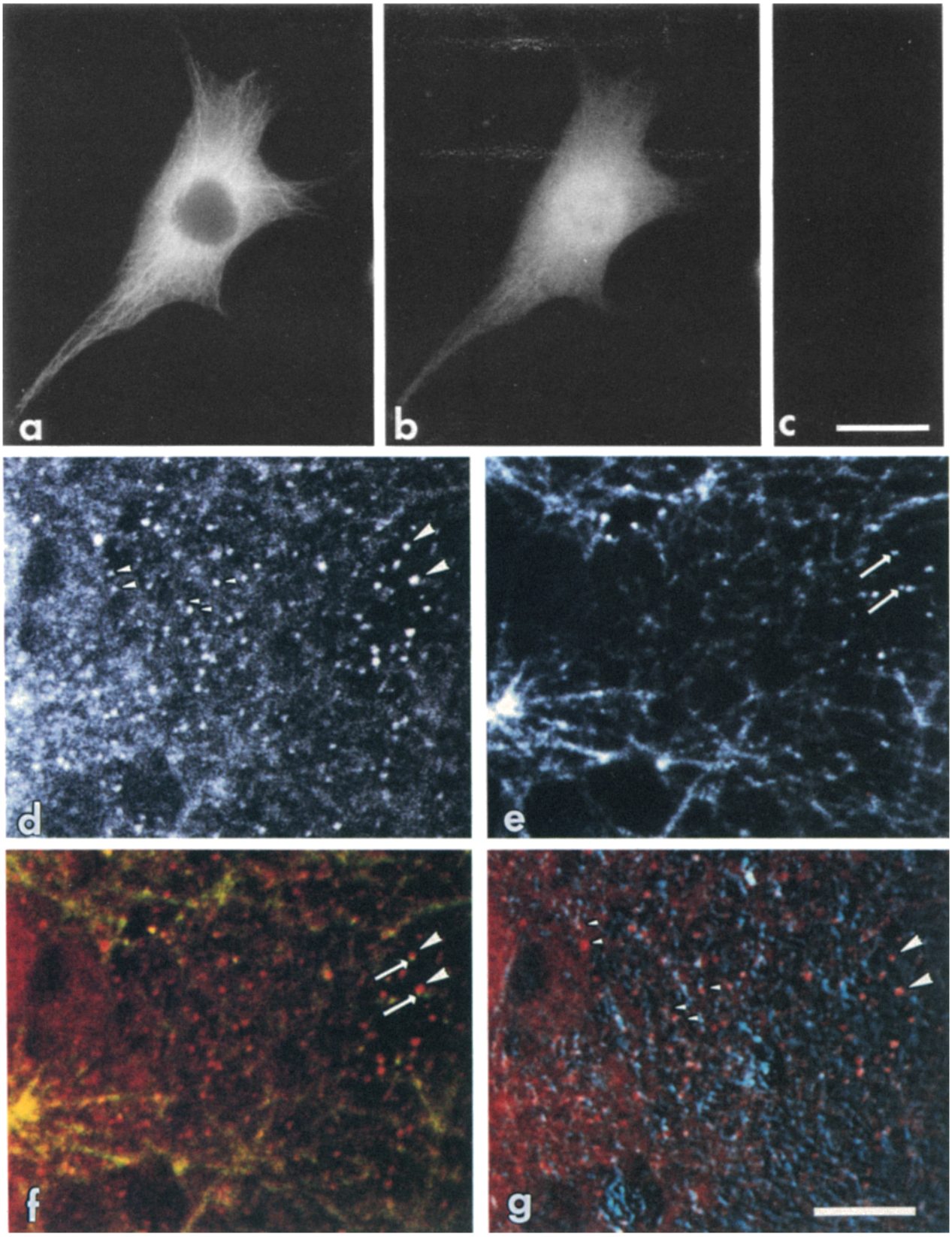

Figure 11. Subcellular localization of KIF4 in interphase L cells. Interphase L cells were double stained with affinity-purified anti-KIF4 antibody (*b* and *d*) and anti-tubulin antibody (*a* and *e*), and were observed by conventional microscopy (*a–c*) and CLSM (*d–g*). With conventional microscopy, anti-KIF4 antibody stained the cytoplasm diffusely with fine punctate and filamentous structures (*b*), while no stain was observed in the control stain with preadsorbed affinity-purified anti-KIF4 antibody supplemented with preimmune sera (*c*). CLSM revealed both the filamentous stain colocalized with microtubules and distinct punctate staining suggesting membranous organelles (*d*, KIF4; *e*, tubulin; *f*, overlay of *d* [red] and *e* [green]). Small arrowheads in *d* (anti-KIF4 staining) and *g* (overlay of *d* [red] and DIC image [blue]) show that the punctate staining colocalized with organelles. Large arrowheads (*d*, *f*, and *g*) indicate organelles adjacent to optically sectioned microtubules (*arrows* in *e* and *f*). Bars: (*c* and *g*) 25 μm.

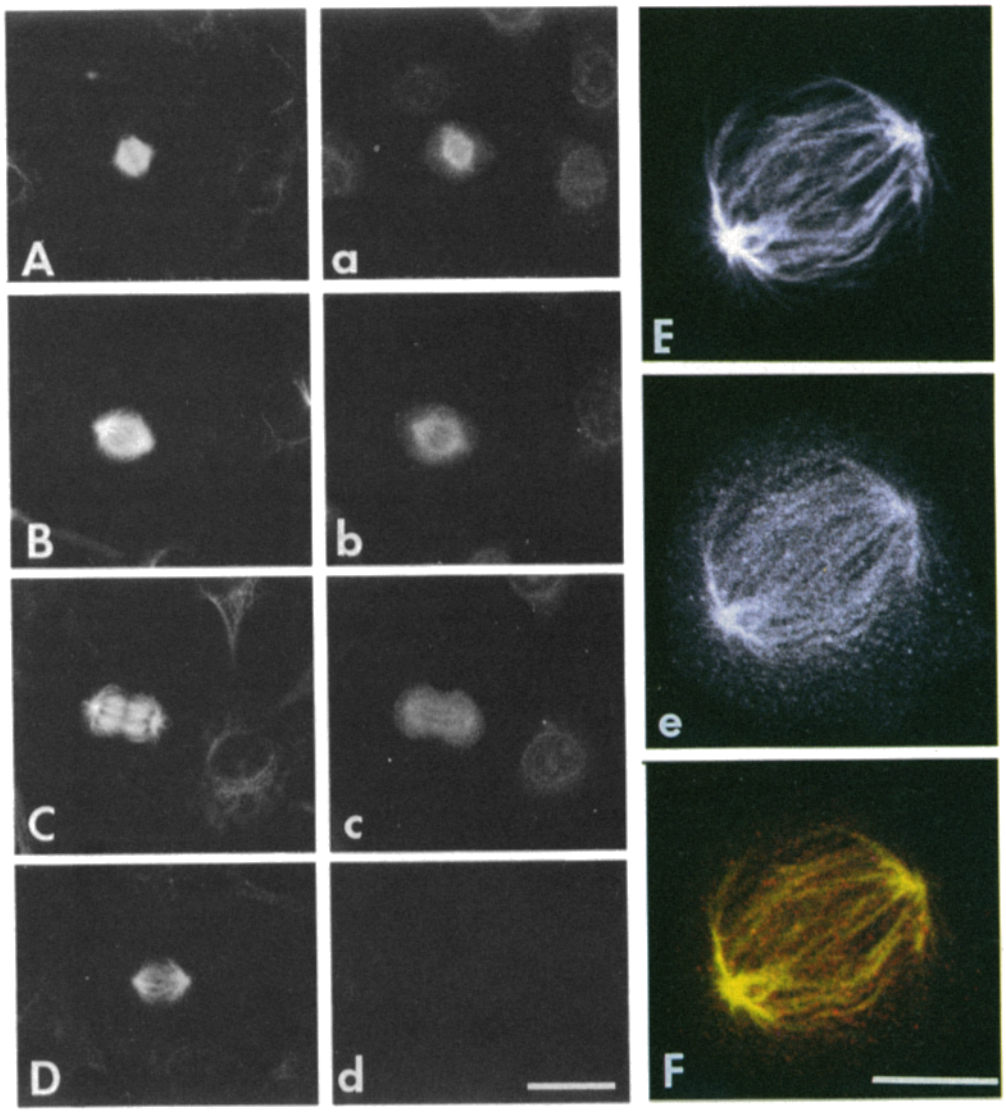

Figure 12. Subcellular localization of KIF4 in mitotic L cells. In mitotic L cells, the cytoplasm and mitotic spindles were stained (*A–E*, tubulin; *a–c* and *e*, KIF4; *d*, preimmune control; *F*, overlay of *e* [red] and *E* [green]), and observed with conventional (*A–D* and *a–d*) and confocal (*E*, *e*, and *F*) microscopes. The stain with anti-KIF4 antibody in the cytoplasm (*a–c* and *e*) was punctate. Spindle microtubules stained by anti-tubulin antibody (*E*) were also stained with anti-KIF4 antibody (*e*) throughout the mitotic phase as shown in *F*. Bars: (*d*) 25 μm; (*F*) 20 μm.

KIF4 Is a Plus-end Directed Microtubule Dependent Motor

In this report, we demonstrated that KIF4 was a motor protein moving toward the plus-end of microtubules. Until now, four other members of the kinesin family have been shown to move on microtubules in vitro. All of the NH_2-terminal motor types, KHC, Eg5, MKLP-1, KIF3A, and KIF4 move on the microtubules to the plus-end. On the other hand, COOH-terminal motor type, ncd, moves on the microtubules to the minus-end (McDonald et al., 1990; Chandra et al., 1993). These data support the idea that the localization of the motor domain in the primary structure and its characteristic sequences determine the direction of transport.

We found that KIF4 induced microtubule bundling in vitro, and that KIF4 partially cosedimented with microtubules even in the presence of ATP, while the addition of KCl increased the release of KIF4 from microtubules. These data suggest that KIF4 may have a nucleotide-insensitive microtubule-binding site other than its motor domain and that this molecule could be able to slide microtubules in opposite directions to each other. The immunofluorescence data on the intracellular localization of KIF4 indicated that some of the protein colocalized with microtubules, especially in mitotic spindles, where microtubules are considered to slide in opposite directions to each other during anaphase B in mitosis. KHC was also shown to bind to microtubules with the tail domain in cells transfected with KHC cDNA (Navone et al., 1992). However, at present we can not exclude the possibility that the lack of light chains or other associated proteins in the baculovirus-expression system artificially caused the ATP-independent interaction of KIF4 with microtubules.

KIF4 Is Expressed Predominantly in Juvenile Tissues and Its Expression Is Controlled Developmentally

The KIF4 transcript was present in juvenile brain but was almost completely absent in adult murine brain. This expression pattern was also the case for other tissues such as kidney, liver, lung, heart, and testis, while spleen expressed KIF4 very strongly both in juvenile and adult mice. This developmentally regulated expression of KIF4 is quite different from the expression of KIF5, a conventional brain-specific KHC, which is expressed in both juvenile and adult brains equally. This regulated expression suggests that KIF4 plays an important role in cell division. This is consistent with the

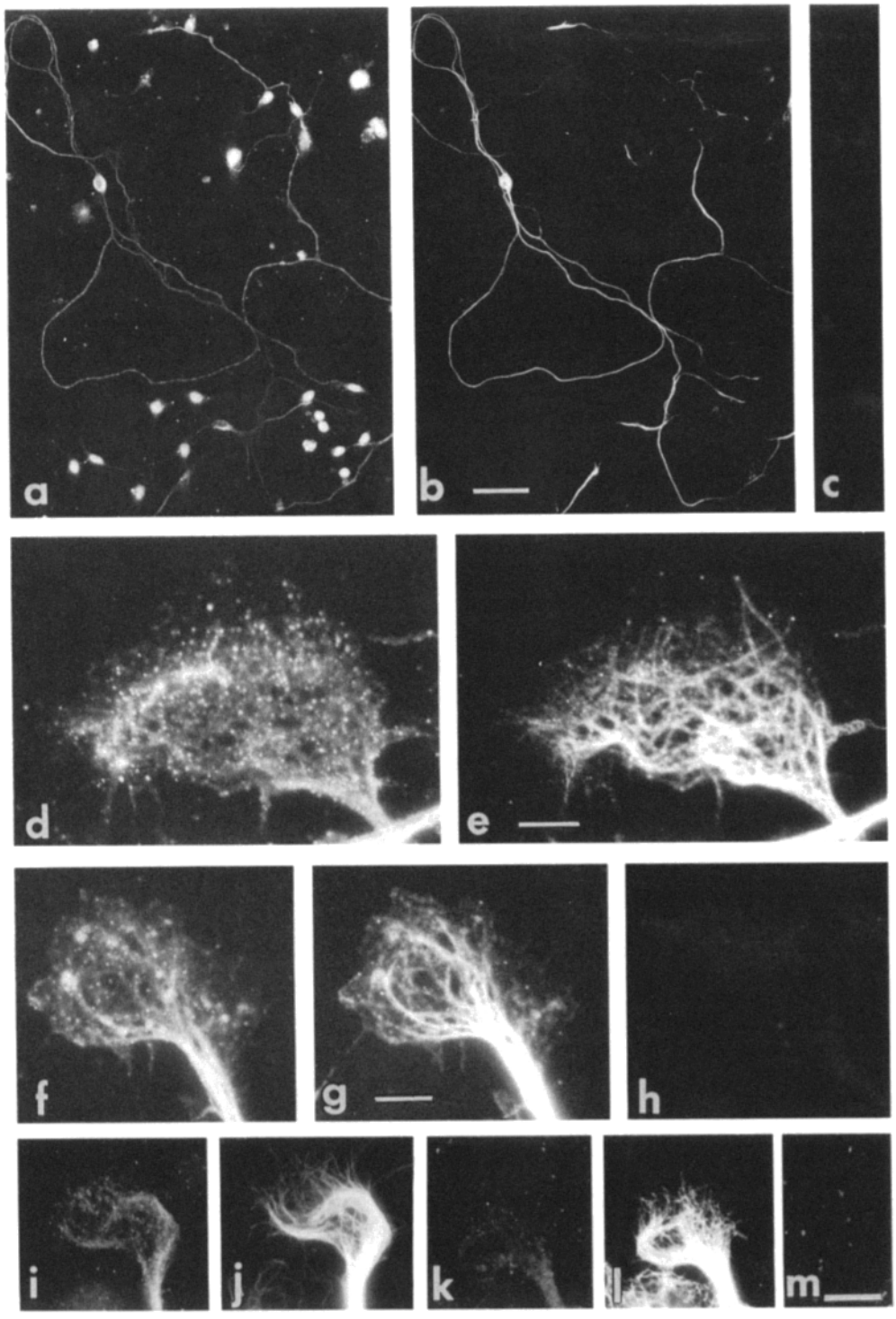

Figure 13. Subcellular localization of KIF4 in P19 cells differentiated into neurons. At 72 h after neural induction, differentiated P19 cells were double-stained with anti-KIF4 (*a*) and anti-neurofilament (*b*) antibodies. Preimmune serum stained nothing (*c*). At 48 h after induction, large, active growth cones of differentiated P19 cells were stained with anti-KIF4 antibody (*d*, *f*, *i*, and *k*), and anti-tubulin antibody (*e*, *g*, *j*, and *l*), with (*i–m*) or without (*d–h*) saponin extraction before fixation. *h* and *m* are negative controls. In growth cones, punctate pattern of KIF4-staining was remarkable and staining along microtubules was also observed (*d* and *f*). Bars: (*b*) 50 μm; (*e*, *g*, and *m*) 10 μm.

results that KIF4 colocalized with spindle microtubules. Kinesin-related proteins which are involved in mitosis such as cut7+ (Hagan and Yanagida, 1992), Xenopus egg kinesin-related protein Eg5 (Sawin et al., 1992*b*), diatom kinesin-related protein (Hogan et al., 1992), MKLP-1 (Nislow et al., 1992), and CENP-E (Yen et al., 1992) were all colocalized in mitotic spindles or centrosomes. On the other hand, KIF4 expression was prominently decreased in adult testis in which mitotic and meiotic cells are abundant, and KIF4 was expressed strongly in adult spleen where the percentage of dividing cells is not considered higher than other tissues examined. Moreover, we demonstrated that KIF4 was expressed in terminal-differentiated neurons such as inner granule cells in the cerebellar cortex and that KIF4 localized in growth cones and neurites in cultured neuronal cells. These data clearly suggest that KIF4 plays important roles in terminal-differentiated cells as well as in proliferating cells.

KIF4 Associates with Membranous Organelles Both in Mitotic Spindles and Neurites

The intracellular localization of KIF4 studied by immunocytochemistry and subcellular fractionation suggests that KIF4 mainly associates with some membranous organelles. In L cells, at least half of the KIF4 associated with membranous organelles recovered in the microsomal fraction, but not in heavy nor light mitochondrial fractions. We also observed punctate staining of KIF4 in mitotic spindles, where a lot of membranous organelles move dramatically along microtubules. We think it reasonable to speculate that KIF4 could be an organelle transporter in the spindle. This speculation can explain the apparent abundance of KIF4 in juvenile tissues where relocalization of organelles during and after mitosis is needed in the proliferating cells.

During the development of the murine brain, first neurons in the hippocampus are generated from the ventricular germinal zone on embryonic day 10 (E10) in the mouse fetus (Caviness, 1973). Neuron formation in the hippocampal region is then completed before birth (Bayer, 1980). However, neurons in the dentate gyrus continue to be formed until postnatal day 20 (Angevine, 1965). In the cerebellum, undifferentiated neurons in the outer granular layer move through the molecular layer into the inner granular layer, growing and differentiating till postnatal day 15 (Fujita, 1966). Because our in situ hybridization data clearly showed the expression of KIF4 mRNA in hippocampal pyramidal cells and inner granular cells in cerebellum on postnatal day 5, it was concluded that KIF4 mRNA is expressed abundantly in differentiated neurons. This means KIF4 has also a function not related to mitosis.

In cultured neuronal cells, KIF4 exists in both neurites and growth cones. In the latter, KIF4 associated with small membranous organelles. This result suggests that KIF4 transports anterogradely small membranous organelles from cell body to growth cones along microtubules in growing neurites of juvenile neurons.

KIF4 is considered to play a role both in cell division and axonal transport. These diversed functions of the motor protein were also reported in the case of conventional kinesin (Wright et al., 1993). Kinesin was considered to transport precursor membranes of nucleus in mitotic spindles and also transport membranes in neuronal axons. However, judging from the developmentally regulated expression and localization, KIF4 seems to be a unique anterograde motor protein which transports membranous organelles specific in juvenile neurons, but general in nonneuronal cells. We have little data of the cargo of KIF4 until now, but obviously it is an important question that ought to be resolved in near future.

We would like to thank Dr. N. R. Lomax for supplying us with taxol, Dr. K. Yoshimura (Zoological Institute, Faculty of Science, University of Tokyo, Tokyo, Japan) for his generous gift of the chlamydomonas, Mrs. F. Ishidate and H. Aizawa (Zeiss, Tokyo, Japan) for their technical assistance in confocal microscopy, and Ms. H. Sato for her technical assistance with the immunological work.

This work was supported by a special Grant-in-Aid for Scientific Research from the Ministry of Education, Science and Culture of Japan, and a grant from Rikagaku Kenkyujyo, Wako, Japan to N. Hirokawa. Y. Okada was supported by Research Fellowships of the Japan Society for the Promotion of Science for Young Scientists, Japan.

References

Aizawa, H., Y. Sekine, R. Takemura, Z. Zhang, M. Nangaku, and N. Hirokawa. 1992. Kinesin family in murine central nervous system. *J. Cell Biol.* 119:1287–1296.

Angevine, J. B., Jr. 1965. Time of neuron origin in the hippocampal region; an autoradiographic study in the mouse. *Exp. Neurol.* 2 (suppl):1–70.

Bayer, S. A. 1980. Development of the hippocampal region in the rat I. Neurogenesis examined with ^{3}H-thymidine autoradiography. *J. Comp. Neurol.* 190:87–114.

Bloom, G. S., M. C. Wagner, K. K. Pfister, and S. T. Brady. 1988. Native structure and physical properties of bovine brain kinesin and identification of the ATP binding subunit polypeptide. *Biochemistry.* 27:3409–3416.

Bradford, M. M. 1976. A rapid and sensitive method for the quantiation of microgram quantities of protein utilizing the presence of protein-dye binding. *Anal. Biochem.* 72:248–254.

Brady, S. T. 1985. A novel brain ATPase with properties expected for the fast axonal transport motor. *Nature (Lond.).* 317:73–75.

Caviness, V. S., Jr. 1973. Time of neuron origin in the hippocampus and dentate gyrus of normal and reeler mutant mice: an autoradiographic analysis. *J. Comp. Neurol.* 151:113–120.

Chandra, R., E. D. Salmon, H. P. Erickson, A. Lockhart, and S. A. Endow. 1993. Structural and functional domains of the Drosophila ncd microtubule motor protein. *J. Biol. Chem.* 268:9005–9013.

Chou, P. Y., and G. D. Fasman. 1974. Prediction of protein conformation. *Biochemistry.* 13:222–245.

Cole, D. G., W. Z. Cande, R. J. Baskin, D. A. Skoufias, C. J. Hogan, and J. M. Scholey. 1992. Isolation of a sea urchin egg kinesin-related protein using peptide antibodies. *J. Cell Sci.* 101:291–301.

Fujita, S., M. Shimada, and T. Nakamura. 1966. ^{3}H-Thymidine autoradiographic studies on the cell proliferation and differentiation in the external and internal granular layers of the mouse cerebellum. *J. Comp. Neurol.* 128: 191–208.

Garnier, J., D. J. Osguthorpe, and B. Robson. 1978. Analysis of the accuracy and implications of simple methods for predicting the secondary structure of globular proteins. *J. Mol. Biol.* 120:97–120.

Goldstein, L. S. B. 1991. The kinesin superfamily: tails of functional redundancy. *Trends Cell Biol.* 1:93–98.

Goldstein, L. S. B. 1993. With apologies to Scheherazade: tails of 1001 kinesin motors. *Annu. Rev. Genet.* 27:319–351.

Grafstein, B., and D. S. Forman. 1980. Intracellular transport in neurons. *Physiol. Rev.* 60:1167–1283.

Hagan, I., and M. Yanagida. 1992. Kinesin-related cut7 protein associates with mitotic and meiotic spindles in fission yeast. *Nature (Lond.).* 356:74–76.

Harlow, E., and D. Lane. 1988. Antibodies: a laboratory manual. Cold Spring Harbor Laboratory Press, Cold Spring Harbor, New York 90–91.

Higgins, D. G., A. J. Bleasby, and R. Fuchs. 1992. CLUSTAL V: improved software for multiple sequence alignment. *Comput. Appl. Biosci.* 8: 189–191.

Hirokawa, N. 1982. The crosslinker system between neurofilaments, microtubules and membranous organelles in frog axons revealed by quick freeze, freeze-fracture, deep-etch method. *J. Cell Biol.* 94:129–142.

Hirokawa, N. 1993. Axonal transport and cytoskeleton. *Curr. Opin. Neurobiol.* 3:724–731.

Hirokawa, N., and H. Yorifuji. 1986. Cytoskeletal architecture in the reactivated crayfish axons with special reference to the crossbridges between microtubules and membrane organelles and among microtubules. *Cell Motil. Cytoskeleton.* 6:458–468.

Hirokawa, N., K. K. Pfister, H. Yorifuji, M. C. Wagner, S. T. Brady, and G. S. Bloom. 1989. Submolecular domains of bovine kinesin identified by electron microscopy and monoclonal antibody decoration. *Cell.* 56:867–878.

Hirokawa, N., T. Yoshida, R. Sato-Yoshitake, and T. Kawashima. 1990. Brain dynein (MAP1C) localizes on both anterogradely and retrogradely transported membranous organelles. *J. Cell Biol.* 111:1027–1037.

Hirokawa, N., R. Sato-Yoshitake, N. Kobayashi, K. K. Pfister, G. S. Bloom, and S. T. Brady. 1991. Kinesin associated with anterogradely transported membranous organelles. *J. Cell Biol.* 114:295–302.

Hogan, C. J., L. Stephens, T. Shimizu, and Z. Cande. 1992. Physiological evidence for involvement of a kinesin-related protein during anaphase spindle elongation in diatom central spindles. *J. Cell Biol.* 119:1277–1286.

Howard, J., A. J. Hudspeth, and R. D. Vale. 1989. Movement of microtubule by single kinesin molecules. *Nature (Lond.).* 342:154–158.

Kondo, S., R. Sato-Yoshitake, Y. Noda, H. Aizawa, T. Nakata, Y. Matsuura, and N. Hirokawa. 1994. KIF3A is a new microtubule-based anterograde motor in the nerve axon. *J. Cell Biol.* 125:1095–1107.

Koonce, M. P., P. M. Grissom, and J. R. McIntosh. 1992. Dynein from *Dictyostelium*: primary structure comparisons between a cytoplasmic motor enzyme and flagellar dynein. *J. Cell Biol.* 119:1597–1604.

Kuznetsov, S. A., E. A. Vaisberg, N. A. Shanina, N. N. Magretova, V. Y. Chernyak, and V. I. Gelfand. 1988. The quaternary structure of bovine brain kinesin. *EMBO (Eur. Mol. Biol. Organ.). J.* 7:353–356.

Laemmli, U. K. 1970. Cleavage of structural proteins during the assembly of the head of bacteriophage T4. *Nature (Lond.).* 227:680–685.

Lye, R. J., M. E. Porter, J. M. Scholey, and J. R. McIntosh. 1987. Identification of a microtubule-based cytoplasmic motor in the nematode *C. elegans*. *Cell*. 51:309–318.

Maeda, K., T. Nakata, Y. Noda, R. Sato-Yoshitake, and N. Hirokawa. 1992. Interaction of dynamin with microtubules: its structure and GTPase activity investigated by using highly purified dynamin. *Mol. Biol. Cell*. 3:1181–1194.

Maniatis, T., E. F. Fritsch, and J. Sambrook. 1982. Molecular cloning: a laboratory manual. Cold Spring Harbor Laboratory Press, Cold Spring Harbor, New York. 7.3–7.36.

Matsuura, Y., R. D. Possee, H. A. Overton, and D. H. L. Bishop. 1986. Baculovirus expression vectors: the requirements for high level expression of proteins including glycoproteins. *J. Gen. Virol*. 68:1233–1250.

McDonald, H. B., R. J. Stewart, and L. S. B. Goldstein. 1990. The kinesin-like ncd protein of *Drosophila* is a minus end-directed microtubule motor. *Cell*. 63:1159–1165.

Meluh, P. B., and M. D. Rose. 1990. KAR3, a kinesin-related gene required for yeast nuclear fusion. *Cell*. 60:1029–1041.

Miller, R. H., and R. J. Lasek. 1985. Crossbridges mediate anterograde and retrograde vesicle transport along microtubules in squid axoplasm. *J. Cell Biol*. 101:2181–2193.

Minami, A., B. M. Paschal, M. Mazumdar, and R. B. Vallee. 1993. Molecular cloning of the retrograde transport motor cytoplasmic dynein (MAP1C). *Neuron*. 10:787–796.

Navone, F., J. Niclas, N. Hom-Booher, L. Sparks, H. D. Bernstein, G. McCaffrey, and R. D. Vale. 1992. Cloning and expression of a human kinesin heavy chain gene: interaction of the COOH-terminal domain with cytoplasmic microtubules in transfected CV-1 cells. *J. Cell Biol*. 117:1263–1275.

Nislow, C., V. A. Lombillo, R. Kuriyama, and J. R. McIntosh. 1992. A plus-end-directed motor enzyme that moves antiparallel microtubules in vitro localizes to the interzone of mitotic spindles. *Nature (Lond.)*. 359:543–547.

Olmsted, J. B. 1981. Affinity purification of antibodies from diazotized paper blots of heterogeneous protein samples. *J. Biol. Chem*. 256:11955–11957.

O'Reilly, D. R., L. K. Miller, and V. A. Luckow. 1992. Baculovirus Expression Vectors: a laboratory manual. W. H. Freeman and Company, New York. 109–138.

Paschal, B. M., and R. B. Vallee. 1987. Retrograde transport by the microtubule-associated protein MAP1C. *Nature (Lond.)*. 330:181–183.

Paschal, B. M., and R. B. Vallee. 1993. Microtubule and axoneme gliding assays for force production by microtubule motor proteins. *Methods Cell Biol*. 39:65–74.

Rudnicki, M. A., and M. W. McBurney. 1987. Cell culture methods and induction of differentiation of embryonal carcinoma cell lines. *In* Teratocarcinomas and Embryonic Stem Cells: a Practical Approach. E. J. Robertson, editor. 19–49.

Saitou, N., and M. Nei. 1987. The neighbor-joining method: a new method for reconstructing phylogenetic trees. *Mol. Biol. Evol*. 4:406–425.

Sanger, F., S. Nicklen, and A. R. Coulson. 1977. DNA sequencing with chain-terminating inhibitors. *Proc. Natl. Acad. Sci. USA*. 74:5463–5467.

Saunders, W. S., and M. A. Hoyt. 1992. Kinesin-related proteins required for structural integrity of the mitotic spindle. *Cell*. 70:451–458.

Sawin, K. E., K. LeGuellec, M. Philippe, and T. J. Mitchison. 1992*a*. Mitotic spindle organization by a plus-end-directed microtubule motor. *Nature (Lond.)*. 359:540–543.

Sawin, K. E., T. J. Mitchison, and L. G. Wordeman. 1992*b*. Evidence for kinesin-related proteins in the mitotic apparatus using peptide antibodies. *J. Cell Sci*. 101:303–313.

Schnapp, B. J. 1986. Viewing single microtubules by video light microscopy. *Methods Enzymol*. 134:561–573.

Schnapp, B. J., and T. S. Reese. 1989. Dynein is the motor for retrograde axonal transport of organelles. *Proc. Natl. Acad. Sci. USA*. 86:1548–1552.

Scholey, J. M., M. E. Porter, P. M. Grissom, and J. R. McIntosh. 1985. Identification of kinesin in sea urchin eggs, and evidence for its localization in the mitotic spindle. *Nature (Lond.)*. 318:483–486.

Scholey, J. M., J. Heuser, J. T. Yang, and L. S. B. Goldstein. 1989. Identification of globular mechanochemical heads of kinesin. *Nature (Lond.)*. 338: 355–357.

Schroer, T. A., E. R. Steuer, and M. P. Sheetz. 1989. Cytoplasmic dynein is a minus-end directed motor for membranous organelles. *Cell*. 56:937–946.

Seals, J. R., J. M. McDonald, D. Bruns, and L. Jarett. 1978. A sensitive and precise isotopic assay of ATPase activity. *Anal. Biochem*. 90:785–795.

Shelanski, M. L., F. Gaskin, and C. R. Cantor. 1973. Microtubule assembly in the absence of added nucleotides. *Proc. Natl. Acad. Sci. USA*. 70:765–768.

Studier, F. W., A. H. Rosenberg, J. J. Dunn, and J. W. Dubendorff. 1990. Use of T7 RNA polymerase to direct expression of cloned genes. *Methods Enzymol*. 185:60–89.

Takemura, R., Y. Kanai, and N. Hirokawa. 1991. In situ localization of tau mRNA in developing rat brain. *Neuroscience*. 44:393–407.

Tanaka, Y., K. Kawahata, T. Nakata, and N. Hirokawa. 1992. Chronological expression of microtubule-associated proteins (MAPs) in EC cell P19 after neuronal induction by retinoic acid. *Brain Res*. 596:269–278.

Towbin, H., T. Staehelin, and J. Gordon. 1979. Electrophoretic transfer of proteins from polyacrylamide gels to nitrocellulose sheets: Procedure and some applications. *Proc. Natl. Acad. Sci. USA*. 76:4350–4354.

Vale, R. D., B. J. Schnapp, T. S. Reese, and M. P. Sheetz. 1985*a*. Movement of organelles along filaments dissociated from the axoplasm of the squid giant axon. *Cell*. 40:449–454.

Vale, R. D., B. J. Schnapp, T. S. Reese, and M. P. Sheetz. 1985*b*. Organelle, bead, and microtubule translocations promoted by soluble factors from the squid giant axon. *Cell*. 40:559–569.

Vernos, I., J. Heasman, and C. Wylie. 1993. Multiple kinesin-like transcripts in Xenopus oocytes. *Dev. Biol*. 157:232–239.

Witman, G. B. 1986. Isolation of Chlamydomonas flagella and flagellar axonemes. *Methods Enzymol*. 134:280–290.

Wright, B. D., J. H. Henson, K. P. Wedaman, P. J. Willy, J. N. Morand, and J. M. Scholey. 1991. Subcellular localization and sequence of sea urchin kinesin heavy chain: evidence for its association with membranes in the mitotic apparatus and interphase cytoplasm. *J. Cell Biol*. 113:817–833.

Wright, B. D., M. Terasaki, and J. M. Scholey. 1993. Roles of kinesin and kinesin-like proteins in sea urchin embryonic cell division: evaluation using antibody microinjection. *J. Cell Biol*. 123:681–689.

Yang, J. T., R. A. Laymon, and L. S. B. Goldstein. 1989. A three-domain structure of kinesin heavy chain revealed by DNA sequence and microtubule binding analyses. *Cell*. 56:879–889.

Yang, J. T., W. M. Saxton, R. J. Stewart, E. C. Raff, and L. S. B. Goldstein. 1990. Evidence that the head of kinesin is sufficient for force generation and motility in vitro. *Science (Wash. DC)*. 249:42–47.

Yen, T. J., G. Li, B. T. Schaar, I. Szilak, and D. W. Cleveland. 1992. CENP-E is a putative kinetochore motor that accumulates just before mitosis. *Nature (Lond.)*. 359:536–539.

Zhang, Z., Y. Tanaka, S. Nonaka, H. Aizawa, H. Kawasaki, T. Nakata, and N. Hirokawa. 1993. The primary structure of rat brain (cytoplasmic) dynein heavy chain, a cytoplasmic motor enzyme. *Proc. Natl. Acad. Sci. USA*. 90:7928–7932.